# The nuclear level density of $^{192}$Os($\alpha, d\gamma$)$^{194}$Ir

**S. P. E. Magagula[1,2], M. Wiedeking [1,2,3], L. Pellegri [1,2], B. V. Kheswa [4], A. C. Larsen [5], K. S. Beckmann [5], F. L. Bello Garrote [5], L. Crespo Campo [5], A. Görgen [5], M. Guttormsen [5], I. Kullmann [5], K. L. Malatji [1], V. Modamio [5], T. Renstrøm [5], E. Sahin [5], S. Siem [5], G. M. Tveten [5], F. Zeiser [5], J.E. Midtbø [5]**

[1]SSC laboratory, iThemba LABS, Somerset West 7129, South Africa.
[2]School of Physics, University of the Witwatersrand, Johannesburg 2050, South Africa.
[3]Lawrence Berkeley National Laboratory, Berkeley, California, USA.
[4]Department of Applied Physics and Engineering Mathematics, University of Johannesburg, Doornfontein 2028, South Africa.
[5]Department of Physics, University of Oslo, N-0316 Oslo, Norway.

E-mail: `spemagagula@gmail.com`

**Abstract.** The nuclear level density (NLD) refers to the number of energy levels per unit of excitation energy. In this study, the NLD of the $^{194}$Ir isotope was extracted from coincidence measurements of the $^{192}$Os($\alpha$,d$\gamma$) reaction, using the Oslo Method. The data were obtained from an experiment conducted at the Oslo Cyclotron Laboratory, where a 30 MeV $\alpha$ beam was directed onto the $^{192}$Os target. Particular emphasis is placed on the normalization procedure employed in the extraction of the NLD. Additionally, the pairing energy, which manifests in the structure of the NLD, was determined to be 1.43 MeV.

## 1 Introduction

In nuclear physics and nuclear astrophysics, the nuclear level density (NLD) plays a pivotal role as an input parameter while calculating reaction cross sections with the Hauser Feshbach [1], which are essential for understanding elemental abundances, neutron densities and nucleosynthesis in general. NLD data is an essential component in the design of nuclear power plants [2, 3] and is also used in calculations related to the transmutation of nuclear waste [4]. Because the NLD is a fundamental tool for understanding many complex nuclear phenomena, it must be accurately extracted and as precisely normalized as possible.
In this study, the new experimental NLD of $^{194}$Ir nucleus is obtained using $^{192}$Os($\alpha, d\gamma$)$^{194}$Ir reaction and is presented, along with a detailed explanation of its step-by-step normalization process. The following sections will give details on the experimental set-up, the data analysis, the normalization technique and conclusions drawn from the shape of the measured NLD.

The $^{194}$Ir NLD data will give important information on calculating neutron capture cross sections, which will in turn be useful in determining neutron density around the transitional nuclei region. Since these data will be used to calculate neutron capture cross sections, and these for $^{194}$Ir are well studied. $^{194}$Ir findings will be used for benchmarking other Ir isotopes.

## 2 Experimental details

The experiment was conducted in the year 2017 at the Oslo Cyclotron Laboratory over a period of 5 days. The accelerator MC-35 Scanditronix cyclotron was used, which was coupled to two detector systems: the Silicon Ring (SIRI) [5] particle telescope, used for detecting charged particles, and the CACTUS array, which is a sodium iodide (NaI(Tl)) [6] detector system used for $\gamma$-ray detection.

The SiRi array consists of eight silicon detectors, each comprising a thin front detector (130 $\mu$m) and a thick back detector (1550 $\mu$m ). Each front detector is segmented into eight silicon strips, yielding a total of 64 $\Delta E - E$ silicon detector configurations. At the time of the experiment, the CACTUS array consisted of 26 NaI(Tl) detectors. The experiment used a 30 MeV $\alpha$ beam for the $^{192}$Os$(\alpha, d\gamma)^{194}$Ir. The $^{192}$Os target was taken from a previous experiment [7], hence the contamination observed in the particle spectra, some of which was due to the result of carbon backing since the target oxidized, leading to the $^{16}$O$(\alpha, p\gamma)$ reaction. The target was 99% enriched and self-supported with a thickness of 0.33 mg/cm$^2$. Also, a self-supporting $^{60}$Ni target was placed in the target chamber under similar experimental conditions for 2 hours for the purpose of calibration. From the $^{16}$O$(\alpha, p\gamma)^{19}$F, the $^{19}$F known peaks were also used for calibration.

## 3 Data analysis

The data were analyzed using the Oslo method [8, 9], which is globally recognized in nuclear physics and has been used in various studies [10, 11, 12]. The Oslo method is a combination of techniques that allows users to simultaneously extract the NLD and $\gamma$ ray strength function ($\gamma$-ray SF) from particle - $\gamma$ coincidence data. The particle-$\gamma$ matrix is the starting point of the Oslo method, then a set of procedures [8] are subsequently performed, eventually leading to the desired quantities. There are four main steps to the Oslo method, namely: Unfolding of the coincidence matrix [13], the extraction of primary-$\gamma$ matrix [14], extraction and normalization of the NLD and $\gamma$-ray SF. We assume the the generalized Brink-Axel hypothesis is true, and hence the $\gamma$-ray transmission coefficient ($\mathcal{T}$) is independent of excitation energy, spins and parities of initial and final states, therefore from the first generation matrix $P(E_x, E_\gamma)$ it can be deduced that:

$$P(E, E_\gamma) \sim \mathcal{T}(E_\gamma)\, \rho(E_x - E_\gamma). \tag{1}$$

Here $\rho(E_x - E_\gamma)$ is the NLD at final excitation energy $E_f = E_x - E_\gamma$following the emission of the first $\gamma$-ray. Furthermore, we fit a theoretical first-generation matrix, which is written as a function of NLD and transmission coefficient ($\mathcal{T}$) to the experimental one, using $\chi^2$ minimization in which the NLD and $\mathcal{T}$ are treated as free parameters. Thus, the NLD and $\mathcal{T}$ are simultaneously extracted from the experimental first-generation matrix. [8].

## 4 Results and discussion

The Oslo method gives the shape of the NLD or functional form of $\rho$ and $\mathcal{T}$, this means that it is possible to get infinite fits for one possible solution of the NLD. Hence, to obtain the correct slope and absolute value, the data must be normalized.

The following equation gives the functional form of the NLD [8, 9],

$$\tilde{\rho}(E_x - E_\gamma) = \rho(E_x - E_\gamma) A exp[\alpha(E_x - E_\gamma)]. \tag{2}$$

To normalize the NLD we need to determine the absolute value of $A$ hence, $\rho$ is modified to fit the known discrete states at low energies and resonance spacing data at the neutron separation energy $S_n$, see Fig. 1 and Table 1. The NLD at a given $E_x$ is defined as [15] follows,

$$\rho(E_x) = \frac{\sqrt{\pi}}{12} \frac{exp(2\sqrt{aU})}{a^{1/4} E_x^{5/4}} \frac{1}{\sqrt{2\pi}\sigma}. \tag{3}$$

Where $\sigma$ is the spin cut off parameter and $a$ is the level density parameter [16, 17]. The s-wave resonance spacing $D_0$ is given by

$$\frac{1}{D_0} = \frac{1}{2}[\rho(S_n, J = I + 1/2) + \rho(S_n, J = I - 1/2)]. \tag{4}$$

$I$ is the spin of $^{192}$Os of the ground state in neutron capture reactions. Under the Ansatz that the +$\frac{1}{2}$ and -$\frac{1}{2}$ states contribute equally to NLD at S$_n$ therefore the NLD at S$_n$ is given by [9]

$$\rho(S_n) = \frac{2\sigma^2}{D_0} \frac{1}{(I+1)exp[-(I+1)^2/2\sigma^2] + exp[-I^2/2\sigma^2]}, \tag{5}$$

and $\sigma$ is given at S$_n$ as:

$$\sigma^2 = 0.0146 A^{5/3} \frac{1 + \sqrt{1 + 4a(E_x - E_1)}}{2a}. \tag{6}$$

Here E$_1$ is the free parameter for the energy shift, see Table 1 [16, 17].

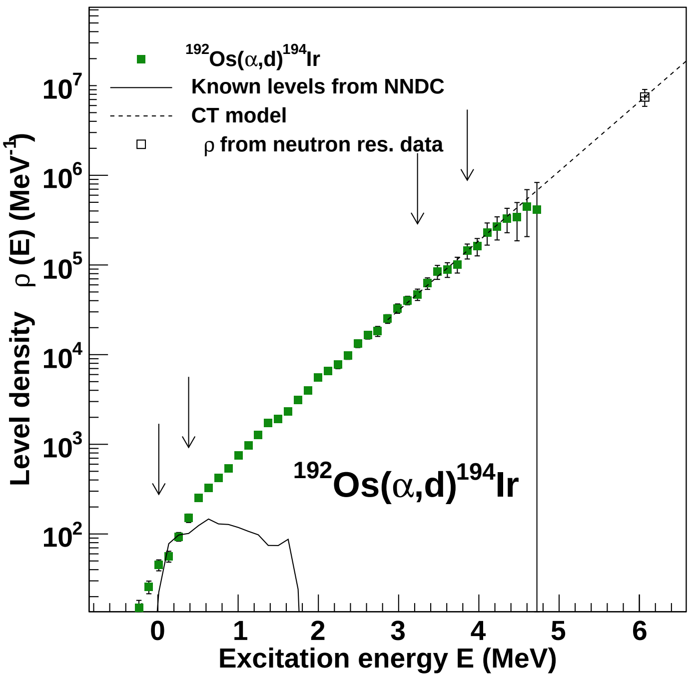


Figure 1: The nuclear level density of $^{192}$Os($\alpha$,d$\gamma$)$^{194}$Ir, the green data points are the Oslo experiment resulting data and the unfilled square is the NLD at neutron separation energy $S_n$ which is calculated using resonance data [18]. The black solid line is the known discrete levels [19]. The dotted black line is the constant temperature interpolation between the experimental NLD and the NLD at $S_n$.

The main results in Fig. 1 show the NLD (green squares) of the $^{194}$Ir that was successfully extracted in this study. The open square, which is the NLD at $S_n$, was calculated as shown by equation 5, with the resonance spacing value taken from Mughabghab [18]. The solid black line shows the known discrete levels taken from NNDC [19]. The two anchor points at low energies normalize the experimental $\rho$ to these discrete levels. Fig. 2 shows the cumulative levels test used to determine the position of the anchor points. The blue line in Fig. 2 represents the cumulative levels of the experimental $\rho$, and the red data is the cumulative level density for discrete levels. Where these two lines diverge is the highest energy that can be used for low-level normalization, which is where the level scheme is considered complete. The black dotted line between experimental $\rho$ and $\rho(S_n)$ is the constant temperature (CT) [20] interpolation at $E_x < 2\triangle$, where $\triangle$ is the paring gap energy.

| **Isotope** | $S_n$ (MeV) | $D_0$ (eV) | $E_1$ (MeV) | $a$(MeV$^{-1}$) | $\rho(S_n)$ (MeV$^{-1}$) |
|---|---|---|---|---|---|
| $^{194}$Ir | 6.067 ± 0.001 MeV | 3.98 ± 0.36 | -1.227 | 17.869 | $7.467\times10^6 \pm 1.591\times10^6$ |

Table 1: Normalization parameters used for the extraction and normalization of the level density, $S_n$ is the neutron separation energy [19], $D_0$ is the resonance spacing from Ref. [18], $a$ is the level density parameter, $E_1$ Fermi-gas shift parameter and $\rho(S_n)$ is the nuclear level density at neutron separation energy.

The anchor points at high energies normalizes the experimental data to the CT model and were placed at $E_x$ = 3.22 and 3.87 MeV above $E_x = 2\triangle$. A slope change is observed around 1.4 MeV in Fig.1, this is believed to be the first pairing gap; the first paring gap energy was calculated and found to be 1.43 MeV. The reason for the change in slope is that most thermal energy is used for pair breaking; hence, there is not enough energy for level excitation. After pair breaking, then the free nucleons get excited to the accessible single-particle states near the Fermi surface, resulting in the exponential rise of the NLD [21]. While there are more pair breaking at higher energies, the feature seems to be stronger at the first pair breaking [22].

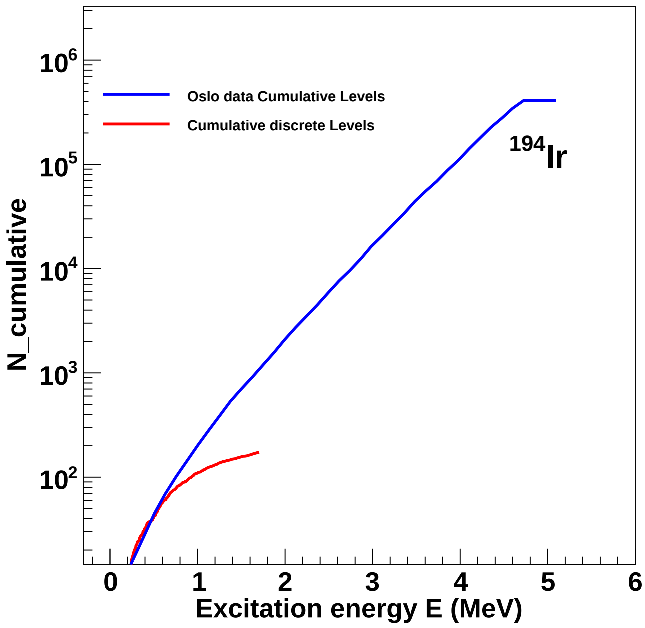


Figure 2: The cumulative levels test to determine low levels normalisation points. Here, the level scheme is considered complete up to an excitation energy of 0.68 MeV.

## 5 Summary and Conclusion

The nuclear level density (NLD) of $^{194}$Ir was successfully measured. A comprehensive normalization was performed using the constant temperature model, known discrete levels, and the level density at the neutron separation energy, $\rho(S_n)$. Furthermore, the first pairing gap energy was observed and determined to be 1.43 MeV. These results contribute to a broader research effort, with related findings presented at the conference. In the future, the normalization method applied in this work will be compared with alternative normalization techniques and resonance data from various sources.

## 6 Acknowledgments

This work is based on research supported in part by the National Research Foundation of South Africa (Grant Number: PMDS22070734847), SAINTS Prestigious Doctoral Scholarship, U.S. Department of Energy, Office of Science, Office of Nuclear Physics under Contract No. DE-AC02-05CH11231, the SARChI under grant No REP-SARC180529336567 and the experiment was financed through ERC-STG-2014 under Grant Agreement No. 637686.

## References

[1] AJ Koning et al. *see also http://www. talys. eu*, 60:211, 2008.

[2] M Ho et al. *Energy Procedia*, 160:459–466, 2019.

[3] Yoshiaki Oka et al. Springer, 2014.

[4] C Rodriguez et al. *Nuclear Engineering and Design*, 222(2-3):299–317, 2003.

[5] M Guttormsen et al. *Nuclear Instruments and Methods in Physics Research Section A: Accelerators, Spectrometers, Detectors and Associated Equipment*, 648(1):168–173, 2011.

[6] M Guttormsen et al. *Physica Scripta*, 1990(T32):54, 1990.

[7] N Nenoff et al. *Nuclear Physics A*, 629(3-4):621–634, 1998.

[8] A Schiller et al. *Nuclear Instruments and Methods in Physics Research Section A: Accelerators, Spectrometers, Detectors and Associated Equipment*, 447(3):498–511, 2000.

[9] AC Larsen et al. *Physical Review C—Nuclear Physics*, 83(3):034315, 2011.

[10] F Giacoppo et al. *Physical Review C*, 91(5):054327, 2015.

[11] M Guttormsen et al. *Physics Letters B*, 816:136206, 2021.

[12] C. P Brits et al. *Physical Review C*, 99(5):054330, 2019.

[13] M Guttormsen et al. *Nuclear Instruments and Methods in Physics Research Section A: Accelerators, Spectrometers, Detectors and Associated Equipment*, 374(3):371–376, 1996.

[14] M Guttormsen et al. *Nuclear Instruments and Methods in Physics Research Section A: Accelerators, Spectrometers, Detectors and Associated Equipment*, 255(3):518–523, 1987.

[15] H. A Bethe. *Physical Review*, 50(4):332, 1936.

[16] T von Egidy and D Bucurescu. *Physical Review C—Nuclear Physics*, 72(4):044311, 2005.

[17] J Zhang et al. *arXiv preprint arXiv:2506.02322*, 2025.

[18] S Mughabghab. In *Atlas of Neutron Resonances*, pages 89–822. Elsevier, Nov 2018.

[19] Brookhaven National Laboratory, USA, as of September 2018. 2019.

[20] A Gilbert et al. *Canadian Journal of Physics*, 43(8):1446–1496, 1965.

[21] K Kaneko et al. *Physical Review C—Nuclear Physics*, 74(2):024325, 2006.

[22] J Wang et al. *Phys. Rev. C*, 111:034324, Mar 2025.